IMAGE FUSION FOR HYPERSPECTRAL IMAGE SUPER-RESOLUTION

Hasan Irmak, Gozde Bozdagi Akar

Middle East Techical University
Dept. of Electrical and Electronics Eng.
Ankara,TURKEY

Seniha Esen Yuksel

Hacettepe University
Dept. of Electrical and Electronics Eng.
Ankara,TURKEY

ABSTRACT

Hyperspectral sensors have high spectral resolution by capturing images in hundreds of bands. Despite the high spectral resolution, low spatial resolution of these sensors restricts the performance of the hyperspectral imaging applications such as target tracking and image classification. Fusing the hyperspectral image (HSI) with higher spatial resolution RGB or multispectral image (MSI) data is a commonly used method in the resolution enhancement of the HSIs. In this paper, we propose a new fusion technique for the HSI super-resolution. The main contribution of this study is formulating the fusion problem in a quadratic manner and also regularizing the solution quadratically using smoothness prior. Moreover, another contribution of the proposed method is converting the fusion problem from spectral domain to the abundance map domain which gives more robust and spectrally consistent results. In the proposed method, first, abundance maps are obtained using linear spectral unmixing and then a quadratic energy function is obtained using these maps and high resolution (HR) RGB image. In addition, quadratic function is regularized using additional constraints. Solving the regularized quadratic function gives the HR abundance maps and these maps are used to reconstruct HR HSI. Experiments show that proposed method yields better performance as compared to state of the art methods in different performance metrics.

Index Terms— Image Fusion, Super-resolution, Hyperspectral, Abundance Maps, Quadratic Optimization

1. INTRODUCTION

Hyperspectral sensors collect hundreds of images in the electromagnetic spectrum and each individual pixel is a complete spectra in the observed spectrum. Therefore, HSI is a three dimensional data cube with two spatial dimension and a spectral dimension. Spectral dimension gives the ability to identify the materials in the scene. Despite the higher spectral resolution, lower spatial resolution of HSIs adversely affects the hyperspectral data processing applications. Super-resolution reconstruction (SRR) techniques can be used in the resolution enhancement of HSIs.

One of the common technique in SRR of HSIs is fusing the HSI with a HR RGB or MSI. In the literature, there are various algorithms for this fusion problem. We can roughly categorize the fusion based methods into two approaches: pan-sharpening methods and subspace based methods [1]. Pan-sharpening is the process of merging HR panchromatic and LR MSIs to create a single HR color image [2]. Similarly, hyperspectral pansharpening aims to combine HSIs and panchromatic images to achieve HR HSI. There are various methods originally designed for MSI pansharpening and adapted to HS pansharpening [3, 4]. On the other hand, there are also methods that are originally designed for HS pansharpening [5, 6]. In [7], there is a good review related to the hyperspectral pansharpening techniques. Subspace based methods is another approach applying a subspace transformation to the both HSI and MSI for the fusion problem. The basis vectors of the transformation can be principal components or the materials of the images. These pure materials are called endmembers and their fractions in a given pixel are called abundance maps. Endmembers are found using spectral unmixing concept. Spectral unmixing is the process of identifying the pure materials and finding the fractions of them in the scene [8]. There are various methods using unmixing concept and abundances of the endmembers in the solution of the fusion problem [9, 10, 11]. One of the advantage of using unmixing is that it gives good and stable solution for the fusion problem [1]. A comparative review for HSI and MSI fusion can be found in [1].

In this paper, we propose a fusion based SRR method for HSIs. First, using the linear spectral unmixing, we convert the SRR problem to the abundance map domain. After LR abundances and spectral signatures of the endmembers are found, using the HR RGB and LR abundances, we define a quadratic problem and extend the problem using a priori information. Moreover, solution space is narrowed down using the properties of the abundances. Jointly solving the quadratic problem gives the HR abundance maps. Finally, using these maps and spectral signatures, we reconstruct the HR HSI. In the next sections, we explain the methodology in detail and give comparative results using real HSIs with different performance metrics.

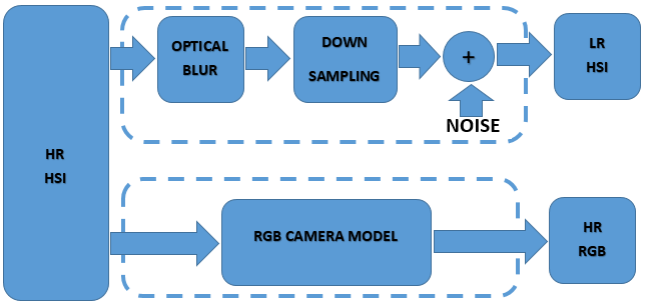

Fig. 1. Observation model used in SRR of HSI

2. METHODOLOGY

Observation model gives the relation between the HR HSI, LR HSI and HR RGB. LR HSI is the spatially down-sampled version of HR HSI whereas HR RGB is the spectrally down-sampled version of HR HSI. A typical observation model can be seen in Figure 1.

Using the Figure 1, the mathematical relation between LR HSI Y_{HSI} and HR HSI Z_{HSI} is:

$$Y_{HSI} = DBZ_{HSI} + n \tag{1}$$

where for p spectral bands, Y_{HSI} and Z_{HSI} are defined as:

$$Z_{HSI} \triangleq \begin{bmatrix} Z(1) & Z(2) & \cdots & Z(p) \end{bmatrix} \tag{2}$$

$$Y_{HSI} \triangleq \begin{bmatrix} Y(1) & Y(2) & \cdots & Y(p) \end{bmatrix} \tag{3}$$

Similarly, relation between HR RGB Z_{RGB} and HR HSI Z_{HSI} is

$$Z_{RGB} = Z_{HSI} R_{RGB}^T \tag{4}$$

In (5),R_{RGB} shows the spectral response function of the RGB image.

Specifically, for the red component of Z_{RGB} (i.e. Z_{RED}), the relation can be written in terms of Z_{HSI} and spectral response function of the red component, R_{RED}:

$$Z_{RED} = Z_{HSI} R_{RED}^T \tag{5}$$

From the linear spectral mixture analysis [8], it is known that HR HS image can be written using abundance maps (A_Z) and spectral signature matrix (P):

$$Z_{RED} = A_Z P R_{RED}^T \tag{6}$$

Equation (6) can be rewritten as in (7).

$$\begin{aligned} Z_{RED} = {} & A_Z(1)(P^T(1))^T R_{RED} + A_Z(2)(P^T(2))^T R_{RED} \\ & + \cdots + A_Z(E)(P^T(E))^T R_{RED} \end{aligned} \tag{7}$$

Using (7) and concatenating the Red, Green and Blue components, (8) is obtained:

$$Z_{RGB} = W_{RGB} z \tag{8}$$

where abundance vector z is defined as:

$$z \triangleq \begin{bmatrix} A_z(1) \\ A_z(2) \\ \vdots \\ A_z(E) \end{bmatrix} \tag{9}$$

After these arrangements, the inverse problem is obtained using the abundance maps and HR RGB image:

$$\widehat{z} = arg\ min_z ||W_{RGB} z - Z_{RGB}||_2^l \tag{10}$$

Similarly, (1) can also be rearranged to a single quadratic function in terms of abundances. Since the problem severely ill-posed, the function should be regularized. In [12], we addressed this problem when there is not any other source of information (i.e. HR RGB or MSI) and only LR HSI is available. Using smoothness prior and inherent properties of abundance maps a single quadratic function is obtained from abundances of LR HSI. A detailed derivation can be found in [12]. In [12], the quadratic function finding HR abundance maps from the LR abundance maps is:

$$\text{minimize} \quad g(z) = \frac{1}{2} z^T H_{MAP} z + f_{MAP}^T z \tag{11}$$

where H_{MAP} and f_{MAP} are defined as:

$$\begin{aligned} H_{MAP} \triangleq {} & 2D_{DB}^T D_{DB} + 2\lambda.[(I - D_{Sx}^1)^T (I - D_{Sx}^1) \\ & + (I - D_{Sx}^{-1})^T (I - D_{Sx}^{-1}) \\ & + (I - D_{Sy}^1)^T (I - D_{Sy}^1) \\ & + (I - D_{Sy}^{-1})^T (I - D_{Sy}^{-1})] \end{aligned} \tag{12}$$

$$f_{MAP} \triangleq (-2y^T D_{DB})^T \tag{13}$$

where D_{Sy}, D_{Sy} and D_{DB} are the horizontal, vertical and blurred-decimation diagonal matrices respectively.

Rewriting (10) in a quadratic form, parameters of the quadratic function for fusion is obtained:

$$H_{fuse} \triangleq 2W_{RGB}^T W_{RGB} \tag{14}$$

$$f_{fuse} \triangleq (-2Z_{RGB}^T W_{RGB})^T \tag{15}$$

Since both MAP and fusion approaches are quadratic, summation is also a quadratic function. Solving the quadratic function gives the HR abundance maps. In the solution of the quadratic function (i.e. HR abundance maps), we used interior point method which has a proven performance in the solution of quadratic functions [13]. Using these HR abundance maps and spectral signatures of the endmembers, final HR HSI reconstructed.

3. EXPERIMENTAL RESULTS

The proposed method is tested using three different remote sensing images, namely Botswana, Pavia and Pavia University [17]. The spatial resolution of the images are 256x256. For the comparison, Lanaras et al.s study is selected [10]. Lanaras et al.s method is a hyperspectral SRR method based on the image fusion of a HR RGB image and a LR HSI; which was shown to have a better performance than several other hyperspectral SR methods [10]. Structural Similarity Index (SSIM), Spectral Angle Mapper (SAM) and Error Relative Global Dimensional Synthesis (ERGAS) are used for the quantitative comparison of the methods.

SSIM is based on the human visual perception which is more sensitive to structural information [14] and is defined as:

$$SSIM(x,y) = \frac{(2\mu_x\mu_y + C_1)(2\sigma_{xy} + C_2)}{(\mu_x{}^2\mu_y{}^2 + C_1)(\sigma_x{}^2 + \sigma_y{}^2 + C_2)} \quad (16)$$

where μ_x and μ_x are the mean values of the pixels in a window for images x and y. σ_x^2, σ_y^2 and σ_{xy} are the variances of x, y and the covariance of x and y respectively. C_1 and C_2 are two constants used to avoid instability, and are set to 0.01 and 0.03 respectively as in [14].

SAM is one of the most common metrics in hyperspectral processing [15]. SAM is the angle between the estimated i^{th} pixel $x(i)$ and the ground truth i^{th} pixel $y(i)$, averaged over the whole image [15]. It measures the average spectral distortion in radians between two images and given in (17) where N is the number of pixels in the image.

$$SAM(x,y) = \frac{1}{N}\sum \arccos \frac{x(i)^T y(i)}{||x(i)||_2 ||y(i)||_2} \quad (17)$$

Last measure is ERGAS which is used to measure the radiometric distortion in the hyperspectral images [16]:

$$ERGAS(x,y) = \frac{100}{SR}\sqrt{\frac{1}{p}\sum_{i=1}^{p}(\frac{RMSE(x_i,y_i)}{\mu_i})^2} \quad (18)$$

where p is the total number of bands, SR is the scale ratio of HSI and MSI spatial resolutions, and μ_i is the average of the i^{th} band.
In these metrics, higher SSIM measures indicate a better match between the estimation and the ground truth. On the other hand, lower SAM and ERGAS values are desired for better match.

The original images form the ground truth and are used to evaluate the performance. The LR HSIs are obtained from the HR images by blurring the HR HSI using a 3x3 uniform kernel, down sampling the result by two and adding 30 dB additive white Gaussian noise signal. Similarly, HR RGB is formed from the original HSI using the spectral response of a typical digital camera.

All three HSI are tested with the above performance metrics. The average of the metric values for all the spectral bands are given in Table I. Visual results are given in Figure 2, 3 and 4. In the visual results, false RGB images are generated using $60^{th}, 70^{th}\, and\, 80^{th}$ bands of the HR HSI.

Table 1. Quantitative Results for different HSIs

	SSIM		SAM		ERGAS	
	Lanaras	Proposed Method	Lanaras	Proposed Method	Lanaras	Proposed Method
Botswana	0,880	0,905	0,056	0,045	13,274	10,881
Pavia	0,859	0,941	0,181	0,096	44,698	24,189
Pavia Univ.	0,857	0,943	0,146	0,074	34,966	18,136
Averages	0,865	0,930	0,128	0,072	30,979	17,735

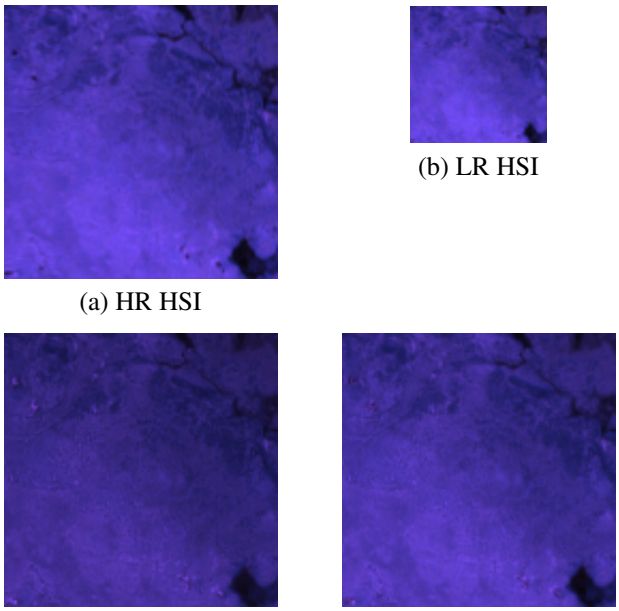

(a) HR HSI (b) LR HSI (c) Lanaras et al. (d) Proposed Method

Fig. 2. Visual Results for Botswana Image

Upon observing the results, in all three HSIs, our proposed method outperforms the Lanaras method in all metrics. Moreover, the visual results are also consistent with the numerical results. Especially in Figure 3 and 4, our proposed method has better performance at the edges of HSIs. Moreover, colors are also more consistent with the HR HSI as compared to Lanaras's method.

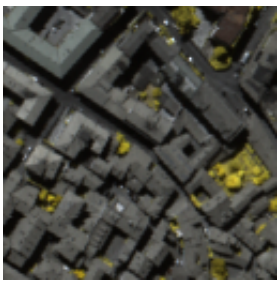

(a) HR HSI

(b) LR HSI

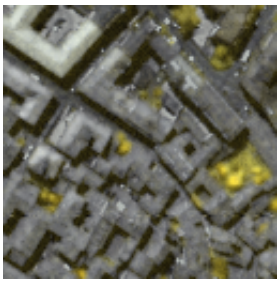

(c) Lanaras et al.

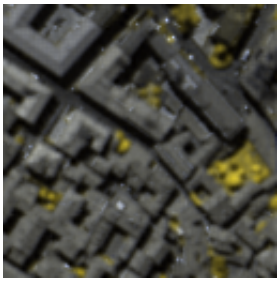

(d) Proposed Method

Fig. 3. Visual Results for Pavia Image

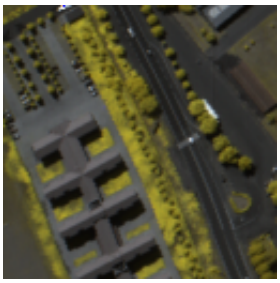

(a) HR HSI

(b) LR HSI

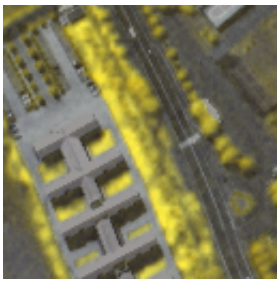

(c) Lanaras et al.

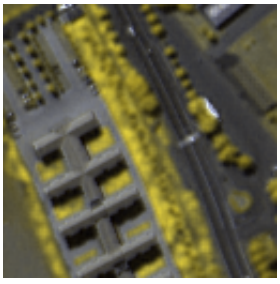

(d) Proposed Method

Fig. 4. Visual Results for Pavia University Image

4. CONCLUSION

In this study, we have proposed a fusion based SRR method for HSIs. This method was applied to fusion of RGB images and HSIs, however, it can be easily extended for fusion of MSIs and HSIs. Proposed method converts the fusion problem to a quadratic optimization problem. Moreover, the solution space is regularized with a priori smoothness information. Optimization problem is defined in the abundance map domain in order to use the information between bands and also decrease the complexity. After finding the HR abundance maps, HR HSI is reconstructed using the HR abundance maps and spectral signatures of the endmembers. Experimental results show that performance of the proposed methods are better than the existing state-of-the-art methods in terms of different performance metrics. Using LR HSI and smoothness prior without RGB image has limited performance compared to fusion based approaches, however, performance is consistent throughout the bands. On the other hand, fusion based approaches have better performance in the matching band range of the auxiliary HR RGB image whereas their performance sharply decreases in the other bands of the spectrum. Proposed fusion approach overcomes the limitations of both mentioned approaches. It has superior performance in all the bands of the spectrum.

5. REFERENCES

[1] Naoto Yokoya, Claas Grohnfeldt, and Jocelyn Chanussot, "Hyperspectral and multispectral data fusion: A comparative review of the recent literature," *IEEE Geoscience and Remote Sensing Magazine*, vol. 5, no. 2, pp. 29–56, 2017.

[2] Gene Rose, "Pan sharpening," *Photogra. Engin. Remote Sens., September*, vol. 17, no. 2, pp. 18–27, 2009.

[3] JG Liu, "Smoothing filter-based intensity modulation: A spectral preserve image fusion technique for improving spatial details," *International Journal of Remote Sensing*, vol. 21, no. 18, pp. 3461–3472, 2000.

[4] Bruno Aiazzi, Stefano Baronti, and Massimo Selva, "Improving component substitution pansharpening through multivariate regression of ms + pan data," *IEEE Transactions on Geoscience and Remote Sensing*, vol. 45, no. 10, pp. 3230–3239, 2007.

[5] Yifan Zhang, Shaohui Mei, and Mingyi He, "Bayesian fusion of hyperspectral and multispectral images using gaussian scale mixture prior," in *Geoscience and Remote Sensing Symposium (IGARSS), 2011 IEEE International*. IEEE, 2011, pp. 2531–2534.

[6] Qi Wei, Nicolas Dobigeon, and Jean-Yves Tourneret, "Bayesian fusion of hyperspectral and multispectral

images," in *Acoustics, Speech and Signal Processing (ICASSP), 2014 IEEE International Conference on*. IEEE, 2014, pp. 3176–3180.

[7] Laetitia Loncan, Luis B de Almeida, José M Bioucas-Dias, Xavier Briottet, Jocelyn Chanussot, Nicolas Dobigeon, Sophie Fabre, Wenzhi Liao, Giorgio A Licciardi, Miguel Simoes, et al., "Hyperspectral pansharpening: A review," *IEEE Geoscience and remote sensing magazine*, vol. 3, no. 3, pp. 27–46, 2015.

[8] Nirmal Keshava, "A survey of spectral unmixing algorithms," *Lincoln Laboratory Journal*, vol. 14, no. 1, pp. 55–78, 2003.

[9] Naoto Yokoya, Takehisa Yairi, and Akira Iwasaki, "Coupled nonnegative matrix factorization unmixing for hyperspectral and multispectral data fusion," *IEEE Transactions on Geoscience and Remote Sensing*, vol. 50, no. 2, pp. 528–537, 2012.

[10] Charis Lanaras, Emmanuel Baltsavias, and Konrad Schindler, "Hyperspectral super-resolution by coupled spectral unmixing," in *Proceedings of the IEEE International Conference on Computer Vision*, 2015, pp. 3586–3594.

[11] Miguel Simões, José Bioucas-Dias, Luis B Almeida, and Jocelyn Chanussot, "A convex formulation for hyperspectral image superresolution via subspace-based regularization," *IEEE Transactions on Geoscience and Remote Sensing*, vol. 53, no. 6, pp. 3373–3388, 2015.

[12] Hasan Irmak, Gozde Bozdagi Akar, and Seniha Esen Yuksel, "A map-based approach for hyperspectral imagery super-resolution," *IEEE Transactions on Image Processing*, 2018.

[13] Thomas Reslow Kruth, "Interior-point algorithms for quadratic programming," M.S. thesis, Technical University of Denmark, DTU, DK-2800 Kgs. Lyngby, Denmark, 2008.

[14] Zhou Wang, Alan C Bovik, Hamid R Sheikh, and Eero P Simoncelli, "Image quality assessment: from error visibility to structural similarity," *IEEE transactions on image processing*, vol. 13, no. 4, pp. 600–612, 2004.

[15] S Rashmi, A Swapna, S Venkat, and S Ravikiran, "Spectral angle mapper algorithm for remote sensing image classification," *IJISET–International Journal of Innovative Science, Engineering & Technology*, vol. 50, no. 4, pp. 201–205, 2014.

[16] Tania Stathaki, *Image fusion: algorithms and applications*, Academic Press, 2011.

[17] Hyperspectral remote sensing scenes. `http://www.ehu.eus/ccwintco/index.php?title=Hyperspectral_Remote_Sensing_Scenes`. (Date last accessed 15-April-2018).